CHEMICAL ENGINEERING TRANSACTIONS

VOL. 67, 2018

A publication of AIDIC
The Italian Association of Chemical Engineering
Online at www.aidic.it/cet

Guest Editors: Valerio Cozzani, Bruno Fabiano, Davide Manca

ISBN 978-88-95608-64-8; **ISSN** 2283-9216

DOI: 10.3303/CET1867082

Enrichment Law of Hazardous Chemicals Enrichment under Dangerous Chemical Environment of Coal Mining

Xiaohua Jin[a], Beifang Gu*[,b]

[a]School of Energy & Environment, Zhongyuan University of Technology, Zhengzhou 451191, China
[b]School of Environmental and Municipal Engineering, North China University of Water Resource and Electric Power, Zhengzhou 450045, China
gbf@ncwu.edu.cn

During the process of coal mining, the CH_4 produced by the coal will be released in the workspace. With the movement of the working face, the overlying strata will be moved or destroyed, resulting in the continuous development of mining cracks and thus the forming a methane enriched area. The study of methane enrichment law is helpful for methane extraction and utilization, and at the same time reduces the risk of workspace. The development of the mining fracture field in overlying strata is determined by the process of overlying strata movement. Since there are many factors affecting the migration of overlying strata, the migration process of the rock strata is complex and the field is limited by many conditions, it is difficult to detect the distribution of the fractured field in the overlying strata. In this paper, the evolution law of mining fracture field will be studied by similar material model test. Based on the geological conditions of the 12# coal seam in Nanzhuang coal mine, Yangquan, the paper uses the similar model test to analyze and discuss the evolution law of the mining fracture field in the overlying strata of the coal seam, which provides a theoretical basis for the design of the mining scheme for the mining in the adjacent layer of the coal seam of the 12# coal seam.

1. Introduction

The fracture development law of the overlying strata in coal seam is analyzed and the gas enrichment area is studied. Based on this, a targeted gas extraction scheme can be put forward, and the problem of gas overrun in the upper corner of the coal mining face with serious gas emission in the adjacent layer can be effectively solved.

Scholars at home and abroad have done a lot of researches on the movement of coal seam overlying strata and the law of fracture development. Liu (1995) have done a lot of theoretical research and measurement on the distribution of water flowing fissures and destroy of overlying strata after coal mining in China (Coal Science Research Institute, 1981; Liu, 1995; Xu, 2004). The distribution of mining fracture in the overlying strata and the breaking of "three vertical zones" and "three horizontal zones" have become the basis for the study of the fracture distribution of the overlying strata in the mining area at present. An empirical formula for calculating the height of water flowing fractured zone is obtained.

In terms of studying the dynamic development law of mining fracture in overlying strata, academician Qian Minggao put forward the key layer theory of rock stratum control, which provides a theoretical basis for the deep study of the dynamic process of the rock strata movement and the evolution law of the mining fracture (Qian, 2000; Qian et al., 1996). At the same time, Qian Ming Gao and Miao Xie Xing classified two types of mining cracks formed in the overlying strata after coal mining [4]. On the basis of this, the zone theory of protective zone was put forward by Yu Bufan (1986). With similar experimental method, Qian Gaoming et al study the evolution law of the mining fracture in the overlying strata after the coal seam mining (Xu et al., 2004; Xu and Qian, 1998). Shi et al. (2004) have studied the distribution of the mining fracture in the overlying strata and the flow characteristics of the pressure relief gas in the adjacent layers by the method of field test and numerical simulation, and the extraction method for pressure relief gas is proposed.

Please cite this article as: Jin X., Gu B., 2018, Enrichment law of hazardous chemicals enrichment under dangerous chemical environment of coal mining, Chemical Engineering Transactions, 67, 487-492 DOI: 10.3303/CET1867082

2. Coal Seam Geology and Working Face

This test takes the mining geological conditions of the 12# coal seam in Nanzhuang coal mine as the prototype. The process of simulating the movement, deformation and destruction of the overlying strata in the 12# coal seam during the recovery process of the working face is simulated, and the evolution of the distribution law of the mining fracture field of the overlying strata is explored, providing guidance to the layout of the gas extraction drilling hole on the adjacent layer of the 12# coal seam. Provide guidance. The bottom of the model is the fine sandstone while the top is 3# coal seam roof sandstone. The cumulative height is 107.7m. The column graph of the model is shown in Table 1.

Table 1: Similar model histogram

No.	Lithology	Thickness (m)	Cumulative thickness (m)	No.	Lithology	Thickness (m)	Cumulative thickness(m)
26	Medium sandstone	13.18	107.71	13	9# coal	0.28	41.79
25	3# coal	1.40	94.53	12	mudstone	6.71	41.51
24	sandy mudstone	3.40	93.13	11	Medium sandstone	13.38	34.80
23	Medium sandstone	8.27	89.73	10	10# coal	0.18	21.42
22	fine sandstone	0.97	81.46	9	mudstone	2.86	21.24
21	mudstone	3.76	80.49	8	limestone	1.69	18.38
20	fine sandstone	0.62	76.73	7	11# coal	0.36	16.69
19	sandy mudstone	3.31	76.11	6	fine sandstone	3.80	16.33
18	6# coal	1.49	72.80	5	sandy mudstone	3.00	12.53
17	sandy mudstone	5.44	71.31	4	mudstone	3.00	9.53
16	mudstone	7.84	65.87	3	12# coal	1.22	6.53
15	8# coal	0.31	58.03	2	mudstone	1.98	5.31
14	Medium sandstone	15.93	57.72	1	Fine sandstone	3.33	3.33

The 12# coal seam in Nanzhuang mine is stable, with an average thickness of 1.22 m and an average inclination of about 6°. The design length of the working face is 180m, and the height is 1.5m. The main adjacent coal seams of 12# coal seam are 6# coal seam, 8# coal seam, 9# coal seam, 10# coal seam, 11# coal seam and 13# coal seam, among which the 13# coal seam is the lower adjacent layer while the others are upper adjacent layers. The physical and mechanical parameters of the coal seam on the coal seam are own in Table 2.

Table 2: Overburden physical and mechanical parameters of the 12# coal seam

No.	Lithology	Bulk density (kg/m^3)	Tensile strength (MPa)	Compressive strength (MPa)	Elasticity (GPa)
1	sandy mudstone	2580	2.73	63.90	15.6
2	Medium-grained sandstone	2620	3.09	85.12	25.3
3	Fine-grained sandstone	2650	3.33	99.80	36.2
4	mudstone	2520	1.36	27.95	11.4
5	Limestone	2660	3.75	110.79	39.4
6	Coal	1430	0.89	9.40	3.5

3. Construction of Similar Simulation Experiment Platform

3.1 Equipment and System

The test equipment and system used in this simulation equipment are mainly composed of similar test bed, test data acquisition system and processing system.

(1) Similar simulation test bed

This test adopts the EWM two-dimensional simulation test bed of the Mining Engineering Laboratory of China University of Mining and Technology (Beijing). The size of the test bed is: long * wide* high =4200mm x 250mm x 1700mm.

(2) Data acquisition and processing system
The data collected in this experiment are mainly the displacement of the model, and the data acquisition and post processing of the displacement data are carried out by the "similar model test image acquisition and processing system" developed by the Mechanics Department of Beijing Institute of Technology. The system is based on the "digital marking point algorithm", which is mainly composed of high resolution camera, computer with high performance and large capacity, and graphics processing software. Its working flow and principle are shown in Figure 1. First, using the high resolution CCD camera produced by Imperx company in the United States, the model images are photographed, and then the model images are stored in real-time with high performance and large capacity computer. Finally, the image processing software is used to process the model images to get the displacement data of each mark point and generate the corresponding graphics.

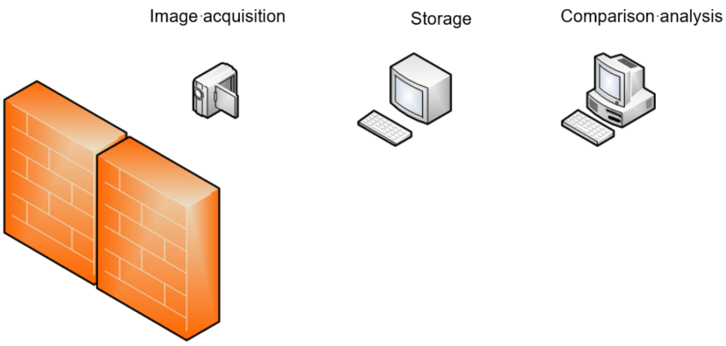

Figure 1: Image acquisition and processing system of similarity model test

3.2 The Determination of Similar Conditions

According to the field condition and the size of the size of the test bed, the similarity constants of the test are as follows: geometric similarity constant $\alpha_l = 100$, bulk density similarity constant $\alpha_\gamma = 1.6$, stress similarity constant $\alpha_\sigma = \alpha_l \times \alpha_\gamma = 160$, elastic modulus similarity constant $\alpha_E = \alpha_\sigma = 160$ and time similarity constant $\alpha_t = \sqrt{\alpha_l} = 10$.
The physical and mechanical parameters of the coal strata in the similar model can be calculated according to the above similarity constants which are shown in Table 3.

Table 3: Rock mass mechanical parameters of each seam in the model

No.	Lithology	Bulk density (kg/m^3)	Tensile strength (MPa)	Compressive strength (MPa)	Elasticity (GPa)
1	sandy mudstone	1612.5	0.01	0.40	97.50
2	Medium-grained sandstone	1637.5	0.01	0.53	158.13
3	Fine-grained sandstone	1656.3	0.02	0.62	226.25
4	mudstone	1575.0	0.01	0.17	71.25
5	Limestone	1662.5	0.02	0.69	246.25
6	Coal	893.8	0.01	0.06	21.88

3.3 Ratio of Similar Materials and model Construction

The similar materials mainly include river sand, gypsum, calcium carbonate and water, in which the river sand is the aggregate, calcium carbonate and gypsum are used as cementing materials to simulate the rock layer according to a certain proportion. In the above materials, a certain proportion of the ink is added to simulate the coal seam, and the mica powder is used to simulate the weak surface of the rock layer, the joint fissure and so on, which are shown in table 4. In the boundary condition, the bottom boundary of the model is a fully constrained boundary, and both sides of the model and the front and rear boundaries are all unilateral constraints.
In the model, the thickness of the simulated coal seam floor is 5.31m, the thickness of the overlying strata is 101.18m, the remaining overlying strata are not laid, and the upper boundary of the model is loaded in the form of uniform load. It is calculated that the uniformly distributed load on the boundary of the model is 0.04MPa. The concrete steps of the model are as follows:
(1) According to the matching plan, the similar materials are weighed and evenly stirred.
(2) Install the two protection boards at the bottom of the test platform.

(3) The mixture of similar materials required for each lamination should be weighed and poured into the middle of the two protective plates of the test platform.
(4) In order to keep the original similar conditions, mica powder is laid on the newly laid layer, which is divided into layers, then pressed and laid down.
(5) Keep going up to the top, and the protection board will rise until all the simulated strata are laid.
(6) Dry the model for two to three days under the protection of the protective plate, then remove the protective plate, and dry it for seven to ten days.

Table 4: Similar material ratio

No.	Lithology	Total Weight (kg)	Component weight(kg)				remark column
			sand	Limestone powder	Gypsum	water	
26	Medium sandstone	32.32	29.09	2.26	0.97	2.26	
25	3# coal	13.14	11.94	0.72	0.48	0.92	
24	sandy mudstone	28.78	25.90	1.73	1.15	2.01	
23	Medium sandstone	35.55	31.99	2.49	1.07	2.49	
22	fine sandstone	16.87	13.50	1.01	2.36	1.18	
21	mudstone	31.09	28.26	2.26	0.57	2.18	
20	fine sandstone	10.78	8.63	0.65	1.51	0.75	
19	sandy mudstone	28.02	25.22	1.68	1.12	1.96	
18	6# coal	13.98	12.71	0.76	0.51	0.98	
17	sandy mudstone	30.70	27.63	1.84	1.23	2.15	
16	mudstone	32.41	29.47	2.36	0.59	2.27	
15	8# coal	2.91	2.64	0.16	0.11	0.20	
14	Medium sandstone	34.22	30.79	2.40	1.03	2.40	key strata III
13	9# coal	2.63	2.39	0.14	0.10	0.18	
12	mudstone	27.74	25.22	2.02	0.50	1.94	
11	Medium sandstone	32.86	29.57	2.30	0.99	2.30	key strata II
10	10# coal	1.69	1.54	0.09	0.06	0.12	
9	mudstone	23.65	21.50	1.72	0.43	1.66	
8	limestone	29.50	25.81	2.21	1.48	1.81	
7	11# coal	3.38	3.07	0.18	0.12	0.24	
6	fine sandstone	33.04	26.43	1.98	4.63	2.31	key strata I
5	sandy mudstone	25.40	22.86	1.52	1.02	1.78	
4	mudstone	24.81	22.55	1.80	0.45	1.74	
3	12# coal	13.14	11.94	0.72	0.48	0.92	
2	mudstone	32.74	29.77	2.38	0.60	2.29	
1	Fine sandstone	57.91	46.33	3.47	8.11	4.05	

3.4 Test Data Acquisition

After the model is dry, the displacement measurement points are arranged on the front of the model. The initial position of the shift point and the position after each recovery are recorded by the high resolution camera. Then the displacement data of each displacement measurement point in the photo are obtained by the image processing software. The position of the displacement point is shown in Figure 2.

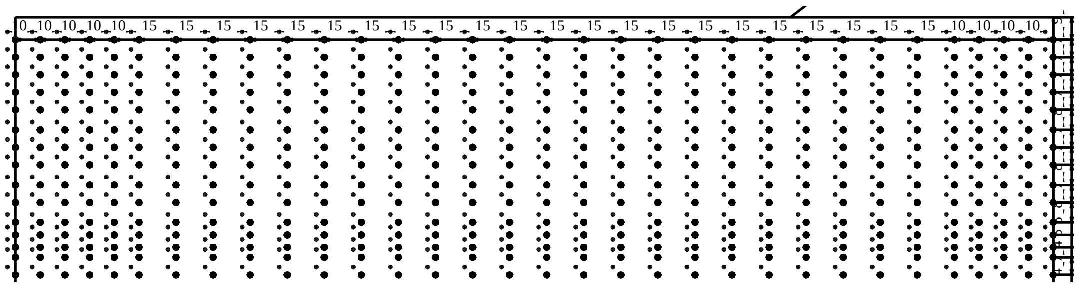

Figure 2: Schematic view of displacement measuring points

After the displacement of the measuring points, the whole model is shown in Figure 3.

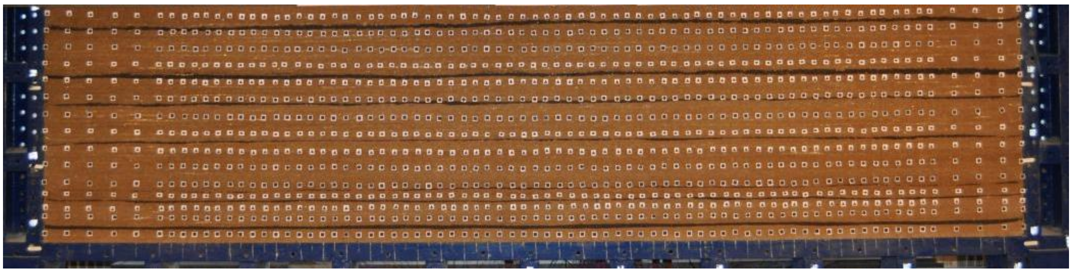

Figure 3: Similar model panorama

4. Experimental results and analysis

After the first fracture of the working face, the deformation of the overlying strata continues, and the mining fractures in the overlying strata gradually begin to develop. The collapse and fracture distribution of overlying strata in normal mining period are shown in Figure 4.

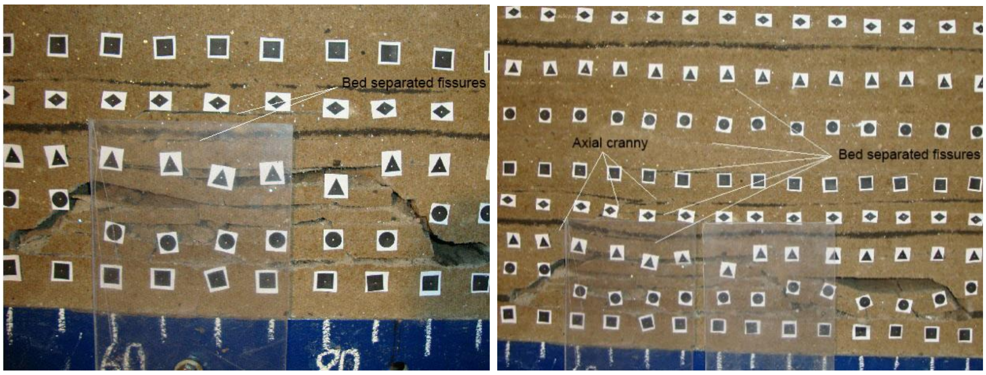

(a) (b)

Figure 4: Overburden collapse fracture distribution form during the normal mining

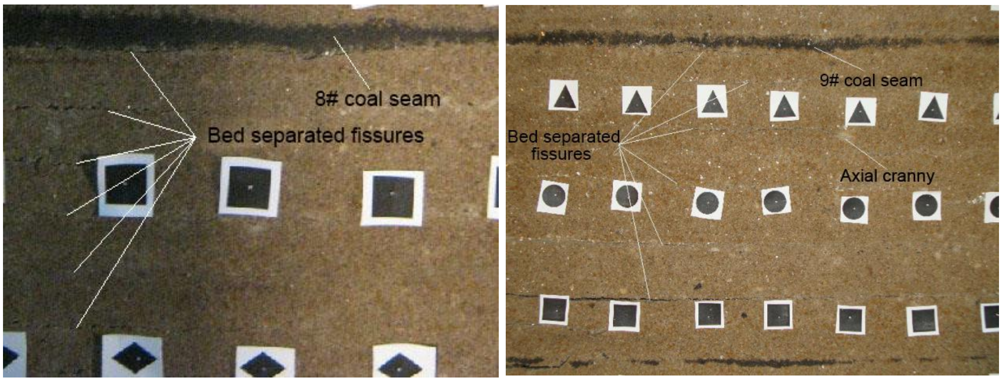

(a) (b)

Figure 5: The fracture distribution form near Coal seam 9#

As shown in Figure 4, as the working face continues to advance, both the direct top and the old top continue to break and fall, and a large number of strata and vertical fractures of the strata appear in the upper strata above, and they are constantly upwards. These separated fissures are the main passageway and the main storage place for the relief gas migration in the upper adjacent layer, which is also conducive to the extraction of the pressure relief gas in the upper adjacent layer. It can be seen from the diagram that the development of mining cracks is lagging behind the working face.

When the working face is pushed forward to 40m, as shown in Figure 4(a), there is an obvious separation crack between the 10# coal seam and the 11# coal seam, which connect 10# and 11# coal seams through the vertical fracture, which is beneficial to the extraction of the pressure relief gas in the coal seam of 10# and 11#. At this time, the upper boundary of the caving zone is 8.2m from the roof of the 12# coal seam, and the upper boundary of the fracture zone is 15.1m from the roof of the 12# coal seam. The breaking angle of the side roof of the open cut is 45°, and the breaking angle of the side wall of the working face is 52°, and there is a vertical crack in the side roof of the coal wall.
When the surface of the working face is advanced to 65m, as shown in Figure 4(b), the abscission layer has been developed up to the 9# coal seam, and the height of the caving zone reaches the maximum value - the upper boundary is 10m to the roof of the 12# coal seam, and the distance between the upper boundary of the crack zone and the 12# coal seam is nearly 35m. At this time, the breaking angle of the roof near the open cut is 45°, and the breaking angle near the coal wall near the working face is 61°.
Figure 5 is the distribution pattern of mining fractures near the 9# coal seam when the working face advances 100m. It can be seen from the figure that the separation and mining cracks are more developed in the 9# coal seam, but only the separations are developed in the area between the 8# and the 9# coal seams, while the development of the vertical penetration cracks is not obvious. The region between the 8# and the 9# coal seams is near the boundary between the fractured zone and the curved subsidence belt. Due to the lack of vertical penetrating fracture which connects the lower fracture zone, the pressure relief gas in the 8# coal seam is stored in these fissures, and the pressure relief gas in the 8# coal seam will not greatly influence the safety production of the working face of the coal seam of the 12#.
According to figure 4 and 5, the maximum distance between the upper boundary of the caving zone and the 12# coal seam is about 10m, and the maximum distance between the upper boundary of the crack zone and the 12# coal seam is about 55m during the advancing process of the working face.

5. Conclusion

Based on the mining geological conditions of the 12# coal seam of Nanzhuang coal mine in Yangquan mining area, a similar model experiment is constructed according to the similarity principle. The similar experiment is based on the mining and geological conditions of the mining face of the 12# coal seam in Nanzhuang coal mine. The experiment was carried out by the EWM 2-D simulation test bed of the Mining Engineering Laboratory of China University of Mining and Technology (Beijing). The collapse morphology and displacement field distribution of overlying strata in the early recovery and normal recovery periods are obtained, and the law of the breakage and subsidence of the key strata is analyzed according to the test phenomenon. At the same time, the range of the “three zones” of the overlying strata is obtained. The distribution of CH_4 in the workspace can be located, thus providing a theoretical guarantee for methane collection.

References

Coal Science Research Institute, 1981, The Laws of Ground Movements and Overburden Failure in Coal Mines and Their Applications, China Coal Industry Publishing House, Beijing, China.
Liu T.Q., 1995, Influence of Mining Activities on Mine Rockmass and Control Engineering, Journal of China Coal Society, 20(1), 1-5.
Qian M.G., 2000, The theory of key strata in ground control, China University of Mining and Technology press, Xu Zhou, China.
Qian M.G., Miao X.X., Xu J.L., 1996, Theoretical Study of Key Stratum in Ground Contral, Journal of China Coal Society, 21(3), 225-230.
Shi B.M., Yu Q.X., Zhou S.N., 2004, Numerical Simulation of Far-Distance Rock Strata Failure and Deformation Caused by Mining Protecting Stratum, Journal of China University of Mining & Technology, 33(3), 259-263.
Xu J.L., 2004, Study and Application of Mining-Induced Fracture Distribution in Green Mining, Journal of China University of Mining & Technology, 33(2), 141-144.
Xu J.L., Qian M.G., 1998, Study on Layout of Grouting Boreholes for Retarding Stratum Subsidence, Journal of China University of Mining & Technology, 27(3), 276-279.
Xu J.L., Qian M.G., Jin H.W., 2004, Study and application of bed separation distribution and development in the process of strata movement, Chinese Journal of Geotechnical Engineering, 5(26), 632-636.
Yu B.F., 1986, Understanding and practice of mining protective layer, Coal Industry Public House, Beijing, China.